Global characteristics of hydrogen-hydrocarbon blended fuels turbulent diffusion flames

Dong, X. [1,*], Ashman, P.J. [1], Nathan. G.J. [2]
Centre for Energy Technology, Schools of [1]Chemical Engineering & [2]Mechanical Engineering,
The University of Adelaide, Adelaide, South Australia, SA 5000, Australia

Abstract
The global performance of a series of attached turbulent diffusion flames using different hydrogen-ethylene fuel blends is reported for H_2 volume fractions varying from 33 to 100%. The parameters assessed are the flame length, radiant fraction and emission indices of NO_x and CO. For blended flames with constant exit strain rate, a transition regime was found for H_2 fractions in the range 50%-65%. Below this range the flames are ethylene dominated while above this they are hydrogen dominated. The normalized flame length, L_f/d_j, decreases with an increasing H_2/mix ratio and this relationship becomes approximately linear as H_2 fraction is varied from 70% to 100%. The NO_x emission index for blended fuels tends to increase with H_2 fraction, although for lower strain rate the trend is reversed for H_2 fractions above 70%. The CO emission index also generally increases with H_2 fraction for ethylene-hydrogen flames, except for very high H_2 fractions, especially for flames with lower strain rate.

Keywords: hydrogen-hydrocarbon blended fuels, turbulent diffusion flames, radiation fraction, pollutant emissions

1. Introduction

There is growing interest in the use of hydrogen as a component in gaseous fuel blends with hydrocarbon fuels because of their complementary nature. Hydrogen can be produced from intermittent renewable energy resources, such as wind and solar, to achieve a near carbon-neutral energy source. Fossil-derived hydrocarbon fuels are usually available at a lower cost and are continuously available but are non-renewable and have a high carbon-intensity. Hence it can be desirable to blend these fuels to achieve continuous supply with a moderate carbon-intensity. In addition, blending can avoid the need to store hydrogen and reduce the risk of flashback [1] thus lowering the cost of use. Furthermore, blending of hydrogen and hydrocarbon fuels may also play an important role in recent technologies such as lean combustion, which suppresses NO_x emissions, since hydrogen extends the lean flammability limit [2]. However, hydrogen and hydrocarbon fuels have very different combustion properties so that variations in the blend ratio will result in the behavior of the resultant flame being different from flames of the pure components. In particular, hydrogen has very much greater flame stability than do hydrocarbon fuels but much lower radiation due to its non-sooting behaviour. The absence of carbon in fuels of pure H_2 has the obvious effect of avoiding the formation of soot; however the impact of H_2 in blended fuels is much more complex. Furthermore, hydrogen has a much higher molecular diffusion, which can result in well-known differential diffusion effects. The combination of these different effects means that it is impossible to determine the influence of hydrogen blending on flame radiation *a priori* and so direct measurements of the combined influences are needed.

Although the global performance of blended fuels has been measured previously, significant gaps remain. Choudhuri *et al.* [3] measured a series of turbulent diffusion flames with a Reynolds number of 8700, while Wu *et al.* [4] reported measurements of the lift-off and blow-off stability limits of pure hydrogen and hydrogen/hydrocarbon mixture jet flames. However, not all of these flames were attached to the burner, which is significant especially for jet burners with small diameters and/or for cases with high exit velocity. Where lift-off occurs it is impossible to isolate the chemical effects due to the addition of H_2 from those of the different physical entrainment mechanisms for lifted and attached flames. Therefore, there remains a need to investigate the effect of varying the hydrogen volume fraction for flames that are all attached. In addition, the hydrogen volume fraction in the previous experiments [5, 6] were no higher than 67%. Furthermore, no previous hydrogen-hydrocarbon flames have been investigated under constant exit strain rate, u/d, which strongly influences the axial and radial soot volume fraction profiles [7, 8]. Therefore, the aim of the current investigation is to assess the effect of hydrogen blend ratio on the global performance of turbulent diffusion flames, using blended C_2H_4 and H_2 fuels with a hydrogen volume fraction ranging from 33% to 100%, at constant exit strain rate.

2. Methodology

The experimental arrangement is shown in Fig. 1. A co-flow burner with a concentric air-jet diameter of 150 mm surrounding a straight tube burner with a nozzle diameter of 4.4 mm and a length of 500 mm was used. The properties and specifications of the C_2H_4 + H_2 blended flames (hereafter referred to as EH flames) are presented in Table 1.

* Corresponding author:
Phone: (+61) 415965728
Email: xue.dong@adelaide.edu.au

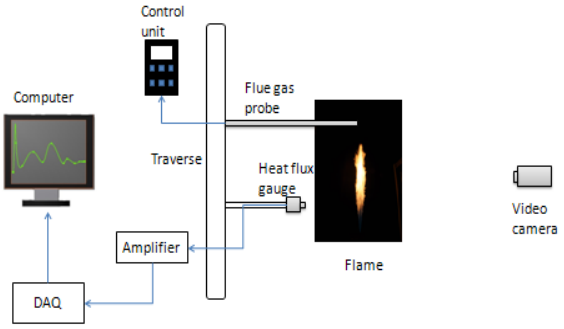

Fig.1. Schematic diagram of the experimental arrangement

2.1 Radiation intensity measurements

A Schmidt-Boelter gauge (manufactured by Medtherm Corporation) was used as the sensor to measure the total radiation from the turbulent diffusion flames. The heat flux sensor is covered with a sapphire window to transmit 76% nominal radiation from 0.6-5 microns, from a view angle of 150 ° [9].

The transducer was positioned at a radial distance of 280 mm from the vertical (x) axis of the flame and traversed parallel to it with ±0.5mm precision. Ten thousand measurements were collected at 1000 Hz and averaged to obtain the radiative flux at each of 25 equi-spaced heights, starting at the nozzle exit plane (±0.5mm) and ending at the flame tip, which was found to be sufficient for statistical convergence [10].

2.2 Flame shape measurement

A tripod-mounted SLR camera (Canon EOS 6D) with a pixel array of 3168 × 4752 and a shutter speed of up to 1/4000 s was used to "freeze" the transient shape of the images. The shape of each flame was averaged from 42 images; the length of the flame from each image is defined as the distance between the burner nozzle and the most downstream flamelet, which is identified in each image by the most downstream pixel cell with intensity larger than 20 (arbitrary unit), similar with the definition of Langman et al [10]. The flame dimensions acquired in this way are repeatable within 3% error.

2.3 Global emission analysis

Global emissions of NO, NO_x, CO and CO_2 were measured continuously for each flame using a Testo 350 flue gas analyzer. The accuracy is ± 10 ppm for CO, ± 2ppm for NO, ± 5 ppm for NOx, and ± 3% of the reading for CO_2. The resolution is 0.01% of the reading for the CO_2 sensor and 0.1 ppm for the other sensors, while the response time for all sensors is less than 40 s. A mixture of the combustion products and ambient air was sampled from above the flame tip. The CO_2 concentration was used to calculate the extent of sample dilution with ambient air. The emission indices of NO_x and CO are presented in g/kJ of energy input from the fuel. All emission indices are estimated to be repeatable to ± 10%.

3. Results and discussion

3.1 Heat flux distribution

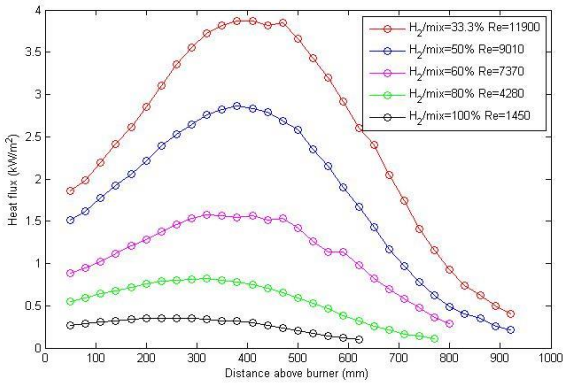

Fig.2. Axial heat flux distribution for varying E:H ratio at constant fuel flow rate (Flame EH_01-EH_05).

Fig. 2 presents the axial heat flux distribution from a series of flames with different ethylene/hydrogen ratios (E:H) but with the same total volumetric flow rate of fuel, and therefore with constant exit strain. The trade-off is that the exit Reynolds number decreases with hydrogen addition, from $Re_0 = \rho Vd/\nu$ = 12,000, which is turbulent, to Re_0= 1,450, which is transitional (Table 1). Hence further work is required to assess the influence of Reynolds number. All of these flames exhibit the well-known trend of heat flux peaking near to the middle of the flame [5, 10, 11]. As expected, the total

Table 1. Specifications and properties of the ethylene-hydrogen blended flames

Flame code	Jet Diameter (mm)	Total flow rate (l/min)	Mixture density (kg/m3)	Mixture viscosity ($kg.m^{-1}.s^{-1}$)	Volume fraction		Strain Rate v/d ($\times 10^3\ s^{-1}$)	Re ($\rho Vd/\nu$)	Air co-flow velocity (m/s)
					C_2H_4/mix (vol%)	H_2/mix (vol%)			
EH_01	4.4	30	0.8157	9.939×10^{-6}	66.7	33.3	7.473	1.19×10^4	0.7
EH_02	4.4	30	0.6340	1.018×10^{-5}	50.0	50.0	7.473	9.01×10^3	0.7
EH_03	4.4	30	0.5251	1.031×10^{-5}	33.3	66.7	7.473	7.37×10^3	0.7
EH_04	4.4	30	0.3075	1.039×10^{-5}	16.7	83.3	7.473	4.28×10^3	0.7
EH_05	4.4	30	0.0899	9.000×10^{-6}	0.0	100	7.473	1.45×10^3	0.7
EH_06	4.4	45	0.8157	9.939×10^{-6}	66.7	33.3	11.21	1.78×10^4	0.7
EH_07	4.4	45	0.6340	1.018×10^{-5}	50.0	50.0	11.21	1.37×10^4	0.7
EH_08	4.4	45	0.5251	1.031×10^{-5}	33.3	66.7	11.21	1.11×10^4	0.7
EH_09	4.4	45	0.3075	1.039×10^{-5}	16.7	83.3	11.21	6.42×10^3	0.7
EH_10	4.4	45	0.0899	9.000×10^{-6}	0.0	100	11.21	2.18×10^3	0.7

radiant fraction decreases with an increase in hydrogen volume fraction (x_v). This is consistent with the reduction in soot concentration associated with the reduction in the C/H ratio [12]. In addition, the location of the peak radiant fraction for the EH flames is translated further downstream (relative to the flame length) with decreasing E:H ratio. This implies that hydrogen delays the onset of the inception of soot formation, which typically occurs closest to the nozzle [13].

3.2 Radiant fraction

The radiant fraction is defined by (1),

$$\chi_r=\frac{Q_r}{Q_F}=\frac{2\pi R\cdot\int_0^L q"(\dot{x})dx}{m\times\dot{H}HV} \qquad (1)$$

where, Q_r is the total radiated power (kW), Q_F is the total thermal power of the flame (kW), R is the radial distance from the nozzle exit to the transducer, m is the mass flow rate of the fuel (kg/s), and HHV is the higher heating value of the fuel (kJ/kg) [10]. The measured radiative heat flux, $q"(x)$ (kW/m^2), is integrated from the nozzle exit ($x = 0$) to the flame tip ($x = L$).

It is clear from Fig.3 that the radiant fraction of EH flames decreases by two-thirds as x_v is increased from 33% to 100%. This can be attributed to a decrease in the radiant heat flux due to a decrease in both soot and carbon dioxide formation [3].

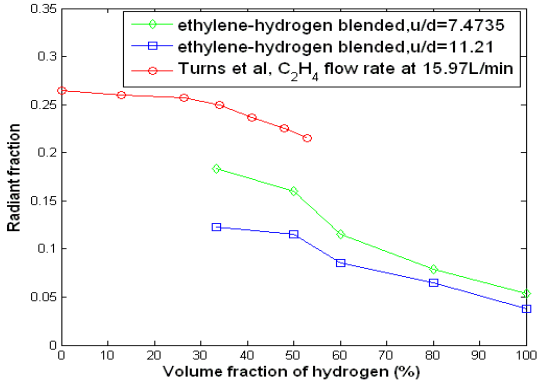

Fig.3. Radiant fraction as a function of H_2 fraction for EH flames (see Table 1 for details) compared with the piloted flames from Turns *et al.* at constant ethylene flow rate [5]. Strain rate u/d is in the unit of 10^3 s^{-1}.

Consistent with previous measurements by Turns *et al.* [5], in which χ_r was found to decrease slightly when hydrogen was added at constant total ethylene flow rate, for the present measurements χ_r was found to decrease dramatically for decreasing E:H at constant *u/d*. Further work is required to determine how much of this difference is due to the influence of the ethylene pilot flame and how much to differences in Reynolds number. It can also be seen that the dependence of χ_r on E:H exhibits two distinct regimes; For blends in which the x_v is less than 50%, the flames are ethylene dominated and the radiation fraction decreases only weakly with a decrease in E:H. However, in the hydrogen dominated regime, i.e. E:H < 0.5, χ_r decreases strongly with further decreases in E:H.

3.3 Flame length

Fig.4. presents the variation in the flame length with the fuel E:H blend ratio. It can be seen that the L_f decreases with an increase in hydrogen fraction, which is consistent with some previous studies [1, 6]. This can be attributed to the increase in the radical pool produced from H_2-O_2-air combustion reaction, such as H and OH radicals, which consequently enhances the burning velocity and thereby reduces the overall flame length [3]. This trend is inconsistent with the measurements of Turns *et al.* [5], which may be because they increased the total flow rate with the increase in hydrogen addition. Also, in contrast with previous experiments, with x_v up to 53% [5, 6] (shown as the red symbols in Fig. 4) the current measurements extend to x_v = 100%, corresponding to pure hydrogen flames. These data show that the normalized flame length, L_f/d_j, decreases linearly with an increase of the hydrogen constituent, except for flames with higher exit strain over the range x_v = 70%-100%, although it should be noted that Re_0 decreases through the transition range for these measurements.

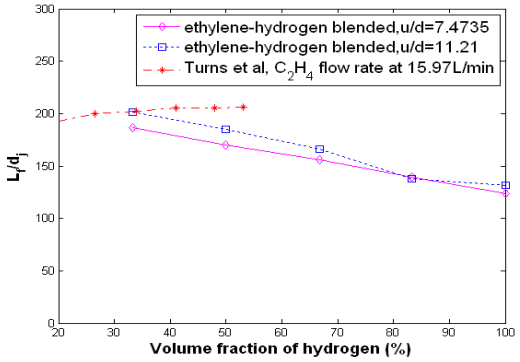

Fig.4. Normalized flame length L_f/d_j as a function of H_2 fraction for EH flames (see Table 1 for flame details), compared with the piloted flames from Turns *et al.* at constant ethylene flow rate [5]. Strain rate u/d is in the unit of 10^3 s^{-1}.

3.3 Emission indices

Emission indices for NO_x and CO were calculated using eqn (2).

$$EI_i = \frac{x_i}{(x_{CO}+x_{CO_2})}\times\left(\frac{n_C\times MW_i}{MW_f\times HHV_f}\right) \qquad (2)$$

where x_i is the mole fraction of species *i* (for *i* = CO or NO_x), x_{CO}, x_{CO_2} are mole fraction of CO and CO_2, n_C is the number of carbon atoms per mole of fuel, MW_i is molecular weight of species *i*, and, MW_f and HHV_f are the molecular weight and higher heating value of the fuel, respectively. Note that emission indices for x_v = 100% were not calculated.

The emission index of NO_x is plotted in Fig. 5 as a function of fuel hydrogen volume fraction. The NO_x

emissions increase with increasing x_v. This can be explained by thermal NOx being the dominant mechanism since the adiabatic flame temperature of H_2 is 114 K higher than that of ethylene and because the radiant fraction decreases with an increase in hydrogen:mix ratio (Fig. 3). This is also consistent with Choudhuri *et al.* [3]. This shows that the trends are dependent on strain-rate and/or Re, so that care should be taken in seeking to generalise these findings.

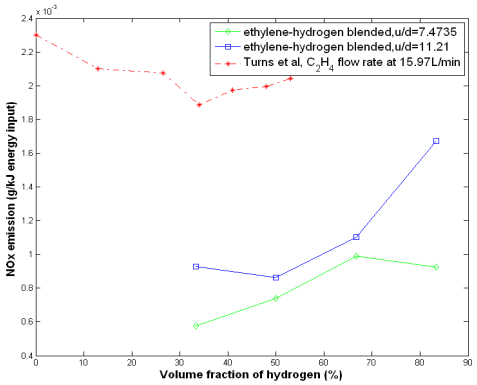

Fig.5. Emission index of NOx as a function of H_2 fraction for EH flames (See Table 1 for flame details)., as compared with the piloted flames from Turns *et al.* at constant ethylene flow rate [5].

The emission index of CO, plotted in Fig. 6 as a function of the fuel E:H blend ratio, increases with H_2 addition up to about x_v = 50%, which is consistent with the observations of Ghafour *et al.* [6]. The overall CO emission is mainly influenced by two competing parameters: i) flame residence time, defined as $T_r=L_f^3/u_j d_j^2$, with shorter residences times inhibiting completion of the CO oxidation process [14], and ii) the carbon input rate – the reduction of which will lower EI_{CO}. For EH flames with higher strain rate, the EI_{CO} is constant for flames with H_2 fraction below 50% but increases as H_2 content increases, corresponding to a decrease in L_f, or rather T_r, which indicates that T_r is the dominant effect on CO emissions for EH flames with higher exit strain rate. On the other hand, for EH flames with lower strain rate, the decrease of carbon input rate balances the effect of the reduction of T_r at H_2 content greater than 50%, which results in a relatively slow growth of EI_{CO} between 50% to70% H_2, and eventually to a decrease of EI_{CO} as x_v exceeds 70%.

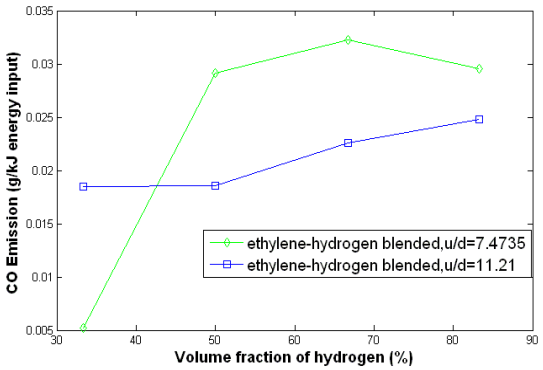

Fig.6. Emission index of CO (EI_{CO}) as a function of H_2 fraction for EH flames (see Table 1 for details).

4. Conclusions

The axial height corresponding to the peak radiation fraction decreases (i.e. moves upstream) as the hydrogen fraction in the fuel mix is increased at constant strain for hydrogen-ethylene fuel blends, but moves downstream relative to the length of the flame.

For ethylene-hydrogen flames, a transition stage was observed for H_2 fractions in the range 50%-65%, below which the flames are ethylene dominated, and above which the flames are hydrogen dominated.

The normalized flame length, L_f/d_j, decreases with an increase of the H_2/mix ratio when the H_2 is added at constant strain, which contrasts earlier work in which it was found to increase when added at constant C_2H_4 flow rate.

The NO_x emission index tends to increase with hydrogen fraction, although the trend reverses at high H_2 fractions at low strain rates suggesting NO_x emissions may be dependent on the exit strain rate.

The CO emission index increases with H_2 fraction for ethylene-hydrogen flames, but with some exceptions in high H_2 fraction region for flames with lower strain rate. The overall EI_{CO} level is determined by the competing impacts of flame residence time and carbon input rate. Nevertheless, it should be noted that the variation in composition at constant strain implies a change in Reynolds number and further work is required to isolate the influence of Reynolds number on the above findings.

5. References

[1] A.R. Choudhuri, S. Gollahalli, International journal of hydrogen energy 25 (2000) 451-462.
[2] A. Katoh, H. Oyama, K. Kitagawa, A.K. GUPTA, Combustion science and technology 178 (2006) 2061-2074.
[3] A.R. Choudhuri, S. Gollahalli, International journal of hydrogen energy 28 (2003) 445-454.
[4] Y. Wu, Y. Lu, I. Al-Rahbi, G. Kalghatgi, International journal of hydrogen energy 34 (2009) 5940-5945.
[5] S.R.a.M. Turns, F.H., Combustion and flame 87 (1991) 319--335.
[6] S. El-Ghafour, A. El-dein, A. Aref, International journal of hydrogen energy 35 (2010) 2556-2565.
[7] J. Kent, S. Bastin, Combustion and flame 56 (1984) 29-42.
[8] N. Qamar, G.J. Nathan, Z.T. Alwahabi, K.D. King, Proceedings of the Combustion Institute 30 (2005) 1493-1500.
[9] Heat Flux Transducers for the Direct Measurement if Heat Transfer Rates, Medtherm Corporation, 1995.
[10] A. Langman, G.J. Nathan, J. Mi, P.J. Ashman, Proceedings of the Combustion Institute 31 (2007) 1599-1607.
[11] J. Gore, G. Faeth, J. Heat Transfer;(United States) 110 (1988).
[12] P. Kumar, D. Mishra, International journal of hydrogen energy 33 (2008) 225-231.
[13] S.-Y. Lee, S.R. Turns, R.J. Santoro, Combustion and flame 156 (2009) 2264-2275.
[14] S.R. Turns, An introduction to combustion, McGraw-hill New York, 1996.